



# Therapeutic effect of the mesenchymal stem cells on vigabatrin-induced retinopathy in adult male albino rat

Ayat Mahmoud Domouky<sup>1</sup>, Walaa M. Samy<sup>2</sup>, Walaa A. Rashad<sup>1</sup>

<sup>1</sup>Department of Human Anatomy & Embryology, Faculty of Medicine, Zagazig University, Zagazig, <sup>2</sup>Department of Medical Biochemistry, Faculty of Medicine, Zagazig University, Zagazig, Egypt

**Abstract:** Vigabatrin (VGB) is an effective antiepileptic drug used mainly to treat infantile spasms and refractory complex partial seizures. However, using VGB was restricted as it was known to cause retinal toxicity that appears as a severe peripheral visual field defect. Accordingly, this study was conducted to examine the histopathological and biochemical effects of VGB on the retina in adult male albino rats and assess the possible therapeutic role of mesenchymal stem cells (MSCs) against this potential toxicity. The rats were divided into three groups (control group, VGB group, and VGB/MSCs group), one week after 65 days of VGB treatment  $\pm$ MSCs. The right eyeballs were prepared for histological and immunohistochemical examination, whereas the left eyeballs were prepared for real-time polymerase chain reaction analysis. Our results demonstrated that MSCs ameliorated retinal pathological changes and downregulated the expression of glial fibrillary acidic protein, vascular endothelial growth factor, and synaptophysin after VGB administration suggesting MSCs function and vascular modulating effect. Moreover, MSCs regulate retinal tissue gene expression of *BAX*, *Bcl-2*, *BDNF*, *NGF*, *synapsin*, *interleukin (IL)-6*, *IL-1 $\beta$* , and *occludin* suggesting MSCs antiapoptotic and immunomodulating effect. In conclusion, MSCs administration could be a suitable therapeutic line to ameliorate VGB-induced retinopathy.

**Key words:** Retina, Brain-derived neurotrophic factor, Nerve growth factor, Synapsins, Synaptophysin

Received January 10, 2022; 1st Revised February 25, 2022; 2nd Revised March 6, 2022; Accepted March 21, 2022


## Introduction

The retina is a very specialized organ formed of ten layers containing many cell types with different morphologies and functions [1]. Given that each retinal layer is critical for capturing and transduction of light signals, damage to any cell layer negatively affects the surrounding cells, manifesting as vision impairment [1]. Many factors, such as vascular

defects, light-induced damage, oxidative stress, damage of blood-retinal barrier, and chemical insults, were suggested to cause progressive retinal damage up to degeneration [2-4].

Vigabatrin (VGB) is an effective antiepileptic drug mainly used to treat infantile spasms and refractory complex partial seizures [5, 6]. Irreversible inhibition of gamma aminobutyric acid transaminase (GABA-T) enzyme is how VGB produces its antiepileptic effect [7, 8]. GABA-T is an enzyme responsible for degrading GABA, a main inhibitory neurotransmitter in central nervous system, resulting in increased GABA levels and consequently decreased neuronal activity and epileptic seizures [9]. However, using VGB was restricted as it was known to cause retinal toxicity that appears as a severe peripheral visual field defect (VFD) [10, 11]. Although retinal toxicity in VGB-treated patients may be

### Corresponding author:

Ayat Mahmoud Domouky 

Department of Human Anatomy & Embryology, Faculty of Medicine,  
Zagazig University, Zagazig 44511, Egypt  
E-mail: amdomouky@medicine.zu.edu.eg

asymptomatic, peripheral VFD is severe in the form of irreversible peripheral vision loss in 30%–50% of adult patients [12, 13], variable degrees of retinal atrophy, and decrease of visual function in 15% of children and 15%–31% of infants [11, 14].

Despite using various methods such as ionizing radiation, laser, or drug treatments for early diagnosis of VFD, their efficiency does not protect against progression to irreversible vision loss. Accordingly, numerous recent studies supported the use of mesenchymal stem cells (MSCs) in treating retinal diseases due to their capacity to regenerate degenerated retinal cells [15–18]. MSCs were considered an appropriate option to treat retinal disorders due to several reasons. First, paracrine signaling causes the repair of neuro-retinal cells by secreting neurotropic factors. Second, immunomodulatory properties of MSCs can decrease the pro-inflammatory microenvironment common to retinal degenerative diseases. Third, their secretion of anti-angiogenic factors responsible for inhibiting proangiogenesis is implicated in the etiology of some ocular diseases [19]. As a consequence, this study was conducted to examine histopathological and biochemical effects of VGB on the retina in adult male albino rats and assess the possible therapeutic role of MSCs against this potential toxicity.

## Materials and Methods

### Chemicals

VGB dissolved in 0.9% NaCl was administered at 40 mg (125 mg/ml) to rats by daily intraperitoneal injection for 65 days, these daily doses (rats: 200 mg/kg) are in-line with those described for the treatment of epilepsy [20].

### Animals

Sixty adult albino rats (190–230 mg body weight) were used in this study divided randomly to 3 groups 20 rats each. They were obtained from the animal house, Faculty of Medicine, Zagazig University. The rats were housed in isolated enclosures (2 rats for each cage) and maintained under standard laboratory and environmental conditions with standard rat chow. All animal experiments were carried out in accordance with the code of ethics of the world medical association and with relevant guidelines and regulations of the institutional animal care and use committee, Zagazig University (ZU-IACUC committee), approval number ZU-IACUC/3/F/92/2021.

### Isolation and characterization of human umbilical cord blood-derived mesenchymal stem cells

Human umbilical cord blood (hUCB) was obtained with informed consent from full-term delivery mothers at Zagazig University Hospital in Zagazig, Egypt. After the placenta was completely separated, UCB was collected under stringent aseptic conditions and drawn into heparinized tubes. The isolation of hUCB-MSCs was done as described previously by Laitinen and Laine [21].

The UCB was then diluted three times in phosphate buffer solution. About 35 ml of diluted cell suspension was added to 15 ml of Ficoll-Paque™ (Lymphocyte Separation Medium 1.077; Lonza Bioproducts, Basel, Switzerland) and centrifuged at 400 g for 20 minutes at 20°C in a swinging bucket rotor. The top layer was then aspirated, leaving just the mononuclear cells (MNC) layer. This MNC layer was put cautiously into a 50 ml conical tube, filled with buffer, mixed, and centrifuged at 300 g for 10 minutes at 20°C. The supernatant MNC was then subcultured in Dulbecco's modified eagle's medium (1.0 g/L glucose, 10% fetal bovine serum, and supplemented with 1% penicillin streptomycin amphotericin B Mixture [10 IU/10 IU/25 mg, 100 ml; Lonza Bioproducts]). Cells were cultured in a CO<sub>2</sub> incubator at 37°C in 5% humidified CO<sub>2</sub> (Heraeus, Langensfeld, Germany). Every two days, non-adherent cells were removed by changing the medium. As a primary culture, the cells were cultivated for two weeks. When adherent cells achieved 80%–90% confluence, they were trypsinized using 0.25% trypsin/ethylene diamine tetra acetic acid and then replated. Experiments were carried out on second-passage cells. MSCs in culture were identified by their adhesiveness and fusiform shape, and through determination of surface markers of hUCB-MSCs using real time polymerase chain reaction (PCR) and flow cytometry. MSCs were labeled with a fluorescence marker using PKH26 Fluorescent Cell Linker Kit (Sigma–Aldrich, St. Louis, MO, USA). Then, labeled MSCs were injected into the rats.

### Experiment protocol

The animal groups classified as following: control group, VGB group, and VGB/MSCs group (20 rats each). Control group was subdivided into vehicle subgroup (10 rats) which received 0.5 ml saline by daily intraperitoneal injection for 65 days and MSCs subgroup (10 rats) which were anaesthetized and injected with hUCB-MSCs “ $2 \times 10^6$  cells in 150  $\mu$ l phosphate buffer solution (PBS)” into the tail vein; VGB group was received 200 mg/kg VGB by daily intraperitoneal

injection for 65 days; and VGB/MSCs group was received 200 mg/kg VGB by daily intraperitoneal injection for 65 days then rats were anaesthetized and injected with hUCB-MSCs “ $2 \times 10^6$  cells in 150  $\mu$ l PBS” into the tail vein.

One week after the MSCs transplantation, rats were examined for general health and body weight were recorded, Intraorbital blood samples were collected, and serum samples were obtained by centrifugation at 3,000 rpm for 20 minutes and kept at ( $-20^{\circ}\text{C}$ ) until assayed. Interleukin (IL)-6 (cat. No. ab222503) and IL-1 $\beta$  (cat. No. ab197742) levels were measured using mouse ELISA kits according to the manufacturer’s protocol.

Rats were anaesthetized intraperitoneally with thiopental (50 mg/kg) and slaughtered, the right eyeballs were harvested, weighted, and immediately immersed and fixed in buffered formalin 10% for H&E, toluidine blue and immunohistochemistry staining. After 24 hours of fixation the eyeballs were further prepared for histopathological examinations. Left eyeballs were dissected, washed with ice-cold saline then retinas were dissected and kept at  $-80^{\circ}\text{C}$  for gene expression analysis.

### ***Histological and morphometric examination***

For H&E and toluidine blue staining, eyeballs specimens were embedded in paraffin after fixation in 10% formalin solution in normal saline. Blocks were sectioned sagittal at eye bulb equator (100–150  $\mu$ m away from the optic nerve) according to Shehata et al. [22], 4–5 microns thickness then they were hoarded on glass slides, deparaffinized for histopathological examination [23]. The slides examined by the light electric microscope (LEICA ICC50 W), Department of Human Anatomy & Embryology, Faculty of Medicine, Zagazig University.

Image analysis software (ImageJ 1.36b, <http://rsbweb.nih.gov/ij>) was utilized to estimate histopathological findings by measuring total retinal thickness ( $\mu$ m), thickness of individual retinal layer ( $\mu$ m), and the number of ganglion cells was counted in in H&E and toluidine blue sections  $400\times$  ( $\times$  counts/field) (1600 $\times$ 1200 pixel), and the average number was taken in each group, only regions with comparative tissue preservation are used for their quantitative analyses. Quantitative data were estimated in 5 separate non-intersected areas for the same slide of each animal, in each animal 5 slides were calculated.

### ***Immunohistochemical examination***

Sequential retinal sections (3  $\mu$ m) were deparaffinized, subsequently endogenous peroxidase satisfying with 3%  $\text{H}_2\text{O}_2$ /methanol for 5 minutes. Sections were applied with primary antibodies overnight at  $4^{\circ}\text{C}$  followed by 1 hour incubation with a biotinylated secondary antibody at room temperature. Antibody binding was pictured by incubating the sections in diaminobenzidine. All incubations were executed in PBS. After all, the sections were counterstained with hematoxylin, dehydrated, and covered. Immunohistochemical staining for anti-GFAP antibody for visualization of glial cells reactivity [24]. The sections were incubated with a primary rabbit polyclonal anti-GFAP antibody (1:1,000,  $4^{\circ}\text{C}$ , overnight; DAKO, Carpinteria, CA, USA), and then with a biotinylated goat antirabbit secondary antibody (DAKO). Immunohistochemical staining for SYN was applied to detect amount of protein in synapse [25]. The sections were incubated with a mouse SYN antibody (Chemicon, Temecula, CA, USA), and then with a biotinylated anti mouse antibody (Vector Laboratories Inc., Burlingame, CA, USA). Immunohistochemical staining for VEGF was performed to detect the vascular integrity and endothelial function [26].

Image analysis software (ImageJ 1.36b, <http://rsbweb.nih.gov/ij>) was utilized to estimate immunohistochemical findings by measuring GFAP and VEGF staining was evaluated based on the percentage of positively stained areas (brown in color) relative to the entire retinal area in each field in  $400\times$  (1600 $\times$ 1200 pixel), the average percentage was taken in each group [27]. The intensity of SYN immunoreactivity was calculated by marking the inner plexiform layer (IPL) & outer plexiform layer (OPL) boundary and measuring the mean gray values after uniform background subtraction [28]. Quantitative data were estimated in 5 separate non-intersected areas for the same slide of each animal, in each animal 5 slides were calculated.

### ***Quantitative real time-polymerase chain reaction***

Total RNA was extracted from retinal tissues using (RNeasy Mini Kit; Qiagen, Hilden, Germany) For evaluating the RNA quality, the A260/A280 ratio was analyzed using the NanoDrop<sup>®</sup> ND-1000 Spectrophotometer (NanoDrop Technologies; Wilmington, DE, USA), followed by cDNA synthesis using the (quantitate Reverse transcription kit; Qiagen). GAPDH was used as an internal standard of mRNA expression. The PCR was performed in 25  $\mu$ l reaction mixture having 50 ng cDNA, 1  $\mu$ l of 10 pM of each primer

**Table 1.** Primer sequence for *BAX*, *Bcl-2*, *BDNF*, *NGF*, *Synapsin*, *IL-6*, *IL-1 $\beta$* , *occludin*, *GAPDH*, *Human GAPDH*, *Human CD105*, and *Human CD34*

Gene	Forward	Reverse
<i>Bax</i>	5'-AGCTCTGAACAGATCATGAAGACA-3'	5'-CTCCATGTTGTTGT CCAGTTC ATC-3'
<i>Bcl-2</i>	5'-GGACAACATCGCTCTGTGGATGA-3'	5'-CAGAGACAGCCAGGAGAAATCAA-3'
<i>BDNF</i>	5'-AAGGTGGATGAGAGTTGAAG-3'	5'-GATGCTGGAAGGTAATGTGT-3'
<i>NGF</i>	5'-TGTGCAGGAGAGATGGATGGT-3'	5'-AGGGCCCCATGATGTGATAC-3'
<i>Synapsin</i>	5'-TGCTGGCGGATCAGCACAAAGT-3'	5'-CCGCACACCGACTGGGCAAAATA-3'
<i>IL-6</i>	5'-CAGCGATGATGCACTGTCAGA-3'	5'-TCCAGAAGACCAGAGCAGATTTTC-3'
<i>IL-1<math>\beta</math></i>	5'-GCTTCAAATCTCACAGCAGCATC-3'	5'-CGTCATCATCCCACGAGTCAC-3'
<i>Occludin</i>	5'-CTCCAACGGCAAAGTGAATG-3'	5'-CGGACAAGTCAGAGGAATC-3'
<i>GAPDH</i>	5'-CGTGTTCCTACCCCAATGT-3'	5'-TGTTCATCATACTGGCAGGTTTCT-3'
<i>Human GAPDH</i>	5'-GGTGAAGTTCGGAGTCAACG-3'	5'-CAAAGTTGTCATGGATGACC-3'
<i>Human CD105</i>	5'-TCCTCCAAGGACACTTGTA-3'	5'-CGCCTCATTGCTGATCATAAC-3'
<i>Human CD34</i>	5'-GGAAGGATGCTGGTCCG-3'	5'-CTGGGGTAGCAGTACCGTTG-3'

IL, interleukin.

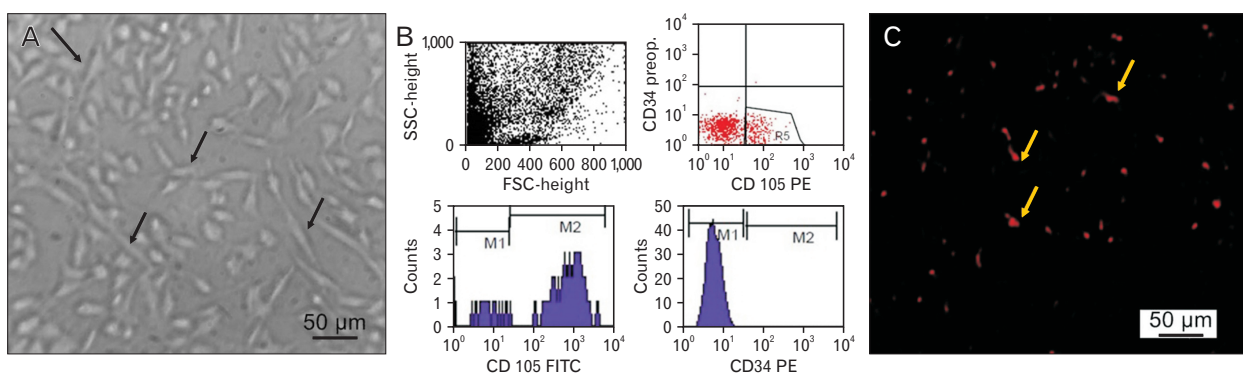


**Fig. 1.** (A) MSCs at day 14 are characterized by their adhesiveness and fusiform shape (black arrows). (B) Flowcytometry charts (M1, negative; M2, positive) show that MSCs express CD105 and don't express CD34. (C) Representative fluorescence micrographs of retina from VGB/MSCs group following MSCs injection showing the homing of MSCs by PKH26 dye (yellow arrows). FITC, fluorescein isothiocyanate; FSC, forward scatter; MSC, mesenchymal stem cells; PE, phycoerythrin; SSC, side scatter; VGB, vigabatrin.

(forward and reverse), and 12.5  $\mu$ l SYBR Green master mix (QuantiTect SYBR Green PCR Kits; Qiagen). Reactions were performed in a real-time PCR (StratageneMx3005P-qPCR System). The amplification program consisted of polymerase activation at 95°C for 5 minutes and 40 cycles of denaturation at 95°C for 1 minutes, annealing at 59°C for 30 seconds and extension at 72°C for 30 seconds. Relative expression levels were normalized and quantified to obtain the  $2^{-\Delta\Delta CT}$  values. The primers used were mentioned in Table 1 [28-30].

### Statistical analysis

The collected biochemical and morphometric data was statistically analyzed using SPSS program (Statistical Package for Social Science) version 18.0 (IBM Corp., Armonk, NY, USA). Descriptive statistics were given as mean $\pm$ standard deviation. One-way ANOVA was used to compare the mean values of different groups. Multiple comparisons were estimated by the least significant difference (LSD) test, a value

of  $P < 0.05$  was statistically significant, a value of  $P < 0.001$  was highly statistically significant, and a value of  $P > 0.05$  was non-statistically significant.

## Results

### Characters and homing of hUCB-MSCs

MSCs in culture were identified by their adhesiveness and fusiform shape. Gene expression analysis for retinal tissue revealed positive expression of non-hematopoietic markers (human CD105) (1.09 $\pm$ 0.15) and negative expression of hematopoietic markers (human CD34) in the MSCs treated groups which was confirmed by flow cytometry. By means of a fluorescent microscope, MSCs treated group showed PKH26 labeled MSCs appearing as bright dots in the retinal tissue, to prove the incorporation of hUCB-MSCs in the retinal tissue after transplantation (Fig. 1).

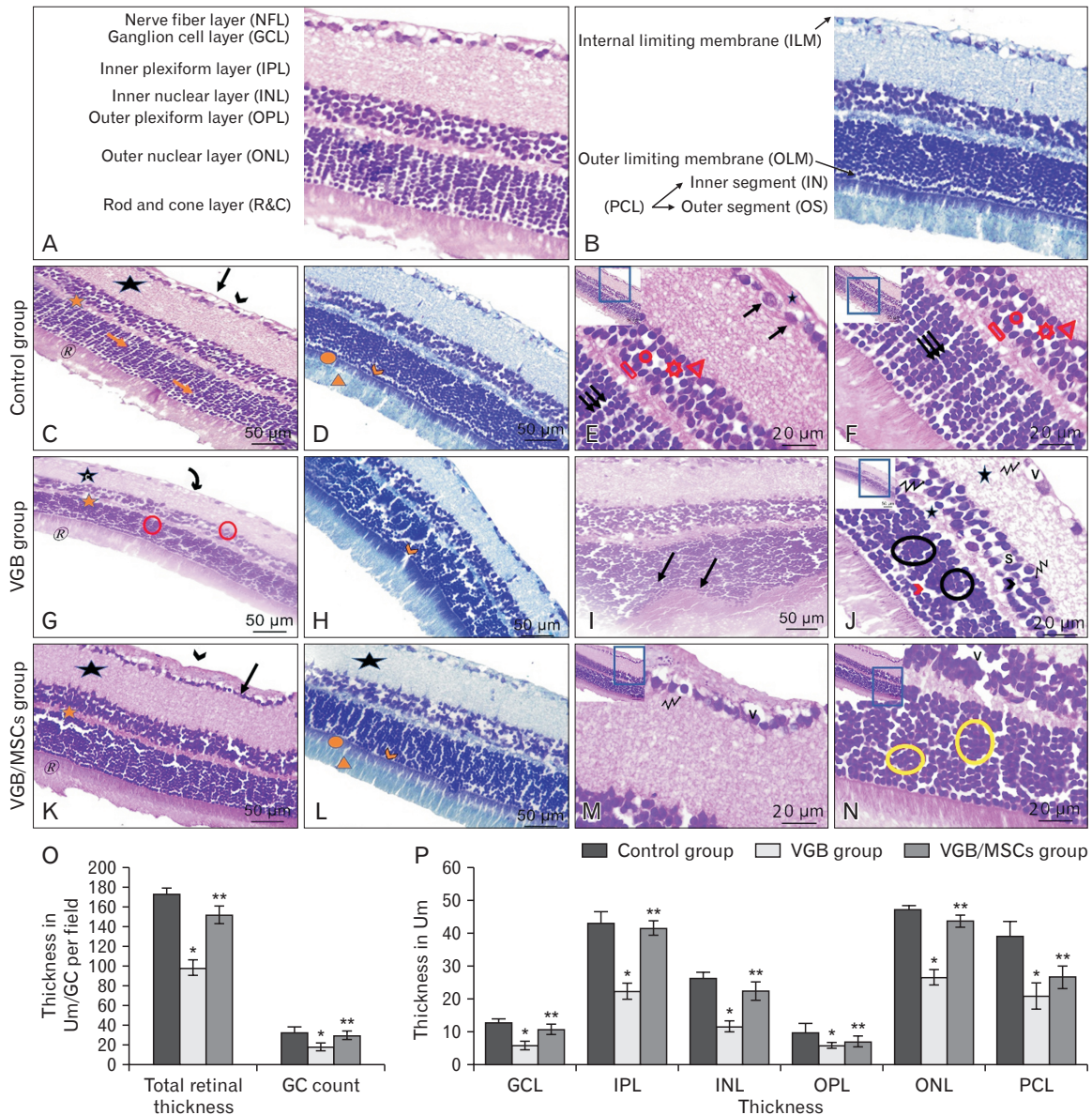


**Fig. 2.** A photomicrograph of a parasagittal section of a rat’s retina (A, C, G, K, I: H&E,  $\times 400$ ; B, D, H, L: toluidine blue,  $\times 400$ ; E, F, J, M, N: H&E,  $\times 1,000$ ), (A, B) showing normal arrangement of the different layers of retina. H&E staining in control group (20 rats), (C) shows GCL formed of a single row of large round to oval cells (arrow) with continued NFL above (arrowhead), IPL and OPL are formed of dense synaptic zone (black and orange stars). INL and ONL are formed of densely dark stained rounded cells arranged mainly in regular rows in control group (orange arrows), R&C is regularly vertical arrangement (®). With toluidine blue staining, (D) shows same histological finding with normal continued OLM (orange arrowheads), inner segment (orange circle) is obviously darker than OS with regular arrangement (orange triangle). In (E, F) GCL is formed of a single row of large ganglion cells exhibiting round to oval, pale, and vesicular nuclei (arrows) with intermingled with nerve fibers (star), INL includes retinal inter-neuronal cell bodies (bipolar cells [red circles], horizontal cells [red rectangles], amacrine cells [red triangles], and Müller glial cells [red pentagon]), ONL arranged normally in regular rows (triple arrows). H&E staining in VGB group (20 rats) (G, I); GCL containing fewer cells (curved arrow), IPL and OPL are less dense synaptic zone (black and orange stars). INL and ONL are arranged in irregular groups (red circles) with marked irregularity at periphery (arrows), R&C is lightly stained (®). With toluidine blue staining, (H) shows discontinued OLM (orange arrowhead). (J) shows degeneration of GCL and NFL and appearance of vacuolation (v) and small dark glial cells (zigzag arrows). The less dense synaptic IPL and OPL well noticeable (black and orange stars). Loss of clear discrimination between types of cells of INL with spaces (s), pyknosis (zigzag arrow), and fragmentation (arrowhead); ONL showing irregular alignments in grouping (circles) with wide spaces (red arrowhead). In VGB/MSCs group (20 rats) (K, L) show same histological features as control, with  $\times 1,000$  mag. (M, N) show GC formed of complete single row of cells with some vacuolation (v) and some dark cell (zigzag arrow), INL includes retinal inter-neuronal cell bodies but disarranged with spaces in between (v), ONL (yellow circles) cells regenerate but still disarranged. Moreover, morphometrical analysis (O, P) in comparing to control group showing that VGB group has a highly significant decrease in total retinal thickness, thicknesses of the individual retinal layers, and in mean ganglion cell count, while in VGB/MSCs group there was no significant different with control group. MSC, mesenchymal stem cells; VGB, vigabatrin; PCL, photoreceptor (rod and cone) cell layer. \*Significant vs control subgroup; \*\*Significant vs VGB group.

### Effect of VGB administration on rat survival rate and body and eyeball weight

All rats were survived all over the experiment. Rats treated with VGB showed no significant difference in body weight  $199.7 \pm 34.4$  g vs.  $210.5 \pm 14.7$  g and  $207.3 \pm 27.6$  g in control and VGB/MSCs groups, respectively. In addition, rats treated with VGB showed significant difference in eyeballs weight  $35.7 \pm 3.9$  mg vs.  $43.6 \pm 4.2$  mg in control group, this

effect is reversed by MSCs treatment as eyeballs weighted  $40.2 \pm 7.3$  mg in VGB/MSCs group.

### MSCs ameliorated retinal pathological changes after VGB administration

Histological retinal examination of control group (20 rats), both vehicle and MSCs subgroups, showed retinal layers which arranged as follow from inner to outer; internal

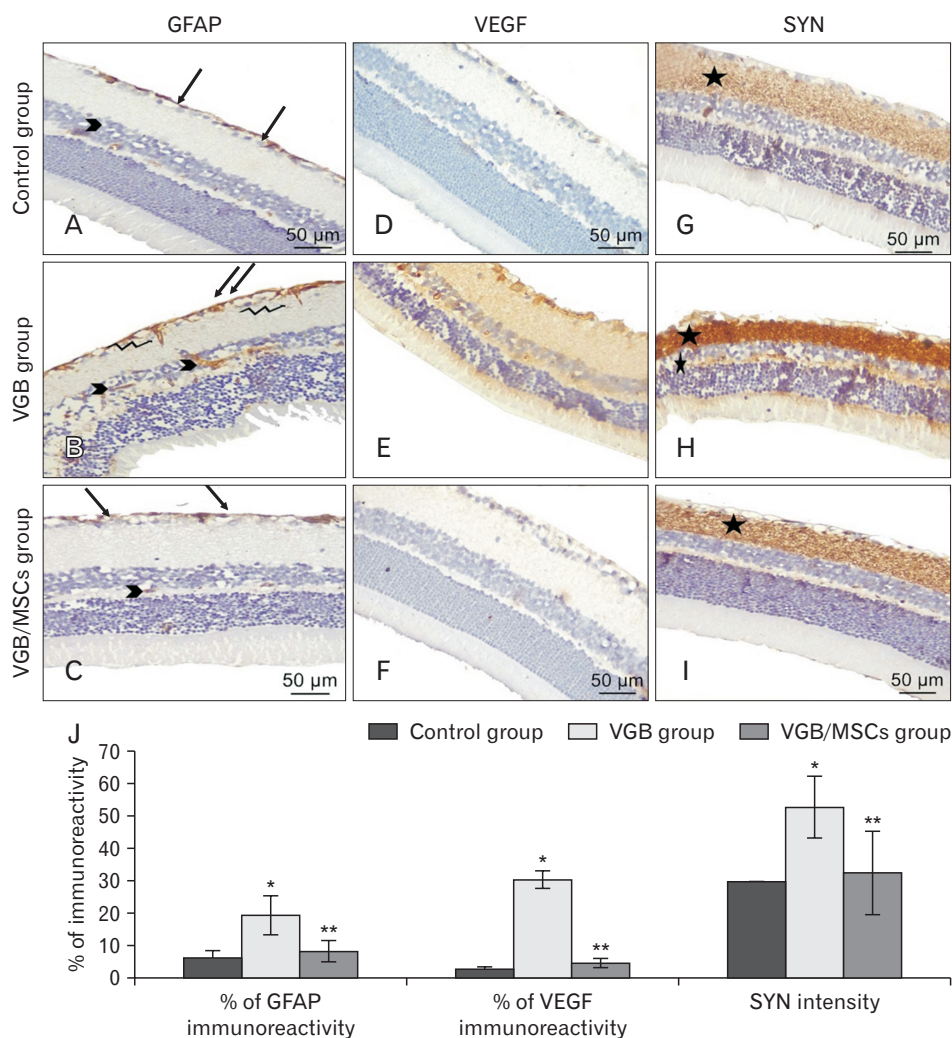


**Fig. 3.** Glial fibrillary acidic protein (GFAP), vascular endothelial growth factor (VEGF), and synaptophysin (SYN) immunohistochemical analysis; GFAP immune-stained sections in control group (20 rats) (A) and VGB/MSCs group (20 rats) (C) limited in the ganglion cell layer (GCL) and nerve fiber layer (NFL) (arrows) and in some Müller glial cell in inner nuclear layer (INL) (arrowheads), in VGB group (20 rats) (B), the immunoreactivity is increased and appeared as marked thickening of NFL (double arrows) with downward indentation (zigzag arrows). VEGF immune-stained sections in control group (D) and VGB/MSCs group (F) revealed negative expression, in VGB group (E) VEGF immunoreactivity showed positive expression in most of the retinal layers. Positive reaction for SYN in the outer plexiform layer (OPL) and the inner plexiform layer (IPL) (stars) was moderately stained in control group (G), strong stained in VGB/MSCs group (I), heavily stained in VGB group (H). (J) Charts demonstrate morphometric analysis of GFAP, SYN, and VEGF expression showing both significant increase in area% immunoreactivity of GFAP and VEGF as well as SYN intensity in VGB group when compared with control group, while, in VGB/MSCs group, MSCs lead to downregulation of GFAP, SYN, and VEGF expression. MSC, mesenchymal stem cells; VGB, vigabatrin. \*Significant vs control subgroup; \*\*Significant vs VGB group.

limiting membrane (ILM), nerve fiber layer (NFL), ganglion cell layer (GCL); formed of a single row of large ganglion cells displaying round to oval, pale and vesicular nuclei with prominent nucleoli and the cells are intermixed with nerve fibers, IPL; includes a thick dense synaptic zone, inner nuclear layer (INL); includes retinal inter-neuronal cell bodies (bipolar cells, horizontal cells, amacrine cells (lightly stained nuclei) and Müller glial cells (star shape cells), OPL; includes a thin dense synaptic zone, outer nuclear layer (ONL); photoreceptor cell bodies arranged regularly vertical, external limiting membrane (ELM), and photoreceptor; rod and cone layer (R&C); formed of inner segment (IS) and outer segment (OS) (Fig. 2C, F).

Histological retinal examination of the VGB group (20 rats) exhibited disorganization of retinal cells and layers; degeneration of ganglion cells and appearance of vacuolation and small dark glial cells in GCL, Loss of clear discrimination between the four types of cells of INL with vacuolations and pyknosis, photoreceptors; rod and cone showed irregular alignments in grouping rather than vertical rows (Fig. 2G, J). Subsequently, retinal examination of the VGB/MSCs group (20 rats) demonstrated a histological picture of the retina nearly comparable to that of control group (Fig. 2K, N).

Morphometrical analysis for total retinal thickness and thicknesses of the individual retinal layers at eye bulb equator in  $\times 400$  magnification fields revealed highly significantly decrease in the retinas of VGB treated rats ( $P < 0.001$ ), compared to control retinas. Also, analysis of mean ganglion cell count revealed significant differences between the groups. In contrast, using MSCs as a therapeutic trial in VGB/MSCs

group showed nearly normal measurement with no significant difference with control group (Fig. 2O, P).

### **MSCs downregulate GFAP, VEGF, and SYN expression after VGB induced retinal pathology**

Immunohistochemical evaluation of GFAP stained sections revealed the GFAP labeling in control group (20 rats) was limited in the astrocytes typically located in the GCL, the NFL and in some Müller glial cell in INL. However, in VGB group (20 rats), there was markedly thickening and increase in staining in the GCL, the NFL with downward indentations. Outcomes of GFAP immunoreactivity in the VGB/MSCs group (20 rats) closely as those of control group (Fig. 3A–C). Examination of VEGF immune-stained sections revealed negative expression in all the retinal layers in control group, and VGB/MSCs group, on the other hand, the retinas in VGB group showed faint positive VEGF immunoreaction distributed in most of the retinal layers (Fig. 3D–F). Additionally, immunohistochemical evaluation of SYN stained sections revealed mild positive reaction in the OPL and IPL in control group, whereas this reaction turned into heavily stained in VGB group. Furthermore, SYN staining of the OPL and IPL was less with MSCs transplantation (Fig. 3G–I).

Additionally, morphometric analysis of GFAP, SYN, and VEGF expression showed both significant increase in area% immunoreactivity of GFAP and VEGF as well as SYN intensity in VGB group when compared with control group ( $P < 0.001$ ), while, in VGB/MSCs group, MSCs led to downregulation of GFAP, SYN, and VEGF expression ( $P < 0.001$ ) (Fig. 3J).

**Table 2.** Biochemical analysis

Gene	Control group (n=20)		VGB group (n=20)	VGB/MSCs group (n=20)	P-value
	Vehicle subgroup	MSC subgroup			
Retinal tissue gene expression in different studied groups					
<i>BAX</i>	1.09±0.18	0.89±0.12	1.63±0.25*	1.31±0.19**	<0.001
<i>Bcl-2</i>	1.11±0.29	1.19±0.13	0.57±0.17*	0.88±0.21**	<0.001
<i>BDNF</i>	1.03±0.17	1.21±0.15	0.48±0.12*	0.76±0.23**	<0.001
<i>NGF</i>	0.99±0.12	1.11±0.07	0.66±0.15*	0.93±0.13**	<0.001
<i>Synapsin</i>	0.97±0.11	1.03±0.09	1.42±0.23*	1.21±0.16**	<0.001
<i>IL-6</i>	1.15±0.12	0.98±0.09	3.09±0.45*	1.56±0.19**	<0.001
<i>IL-1<math>\beta</math></i>	1.13±0.14	0.90±0.11	4.13±0.49*	1.97±0.36**	<0.001
<i>Occludin</i>	1.11±0.19	0.97±0.12	0.43±0.11*	0.81±0.17**	<0.001
Serum inflammatory markers analysis in different studied groups					
<i>IL-6</i>	2.16±0.23	2.03±0.17	39.34±6.24*	23.25±4.25***	<0.001
<i>IL-1<math>\beta</math></i>	4.12±0.36	3.11±0.24	23.14±3.21*	9.34±1.78***	<0.001

MSC, mesenchymal stem cells; VGB, vigabatrin; IL, interleukin. One-way ANOVA, and least significant difference (LSD) test:  $P > 0.05$ , no significant differences;  $P < 0.05$ , significant differences;  $P < 0.001$ , highly significant differences. \*Significant vs. control subgroup; \*\*Significant vs. VGB group.

### ***MSCs' immunomodulated effects in serum samples after VGB administration***

Inflammatory response: gene expression of IL-6 and IL-1 $\beta$  was significantly increased in the VGB group, but significantly decrease in the VGB/MSCs group compared to those treated with VGB only, showing the anti-inflammatory impact of MSCs (Table 2).

### ***MSCs regulate retinal tissue gene expression of BAX, Bcl-2, BDNF, NGF, Synapsin, IL-6, IL-1 $\beta$ and occludin after VGB administration***

Gene expression of occludin was significantly decreased in VGB group while there was significant increase as response to MSCs treatment in VGB/MSCs group. Moreover, gene expression of IL-6 and IL-1 $\beta$  was significantly increased in the VGB group, but significantly decreased in VGB/MSCs group compared to rats treated with VGB only indicating the anti-inflammatory effect of MSCs.

As for apoptosis, VGB group showed significant upregulation in pro-apoptotic gene; BAX mRNA expression besides, significant downregulation in the anti-apoptotic; Bcl-2 mRNA expression in comparison to control group however these results were reversed in the VGB/MSCs group. As for brain-derived neurotrophic factor (BDNF) and nerve growth factor (NGF), there was significant decrease in their mRNA expression levels in VGB group compared to control group while there was significant increase in their expression in VGB/MSCs group compared to VGB group. Moreover, there was significant upregulation in *Synapsin* gene expression in VGB group compared to control and there was significant decrease in its expression in VGB/MSCs group compared to VGB group. As regarding to control group, usage of MSCs in MSCs subgroup showed decrease in BAX and increase Bcl-2, BDNF, NGF and Synapsin in comparison to vehicle subgroup however it wasn't statistically significant (Table 2).

## **Discussion**

Although VGB is rapid acting, highly effective, and presented a major contribution as the first line monotherapy in treating infantile spasms [31], retinal toxicity development as one of the most concerning adverse effects was an alarm to limit its use. Accordingly, this study aimed to shed light on this retinal toxicity and assess the role of MSCs in treating VGB-induced retinal insult.

In this study, the histopathological findings in VGB treat-

ed group included disorganization of retinal cells and layers, degeneration of ganglion cells and appearance of vacuolation and small dark glial cells in GCL, loss of clear discrimination between the four types of cells of INL with vacuolations and pyknosis, and irregular alignments in the ONL in grouping rather than vertical rows. These results agreed with Duboc et al. [32], who recorded that VGB caused ONL disorganization and confirmed by Jammoul et al. [33], who added disruption of GCL and shortening of the outer and inner cone segments [20]. Moreover, Wang et al. [34] confirmed that VGB caused R&C disorganization and cone damage.

In addition, eyeballs' weight and morphometrical analysis at eyeball equator revealed a highly significant decrease in eyeballs' weight, total retinal thickness, thicknesses of individual retinal layers, and decrease of mean ganglion cells count in VGB treated group compared to other groups. This change was noticeable in the absence of body weight change, eliminating the contribution of any systemic effects following intraperitoneal injection of VGB. This was in accordance with a previous work that studied the toxic effect of glutamate on the retina [26].

Increased immunoreactivity for GFAP and SYN with positive VEGF immunoreaction in VGB treated group were corroborated by morphometric analysis. The finding regarding GFAP immunoreactivity copes with Gaucher et al. and Zhou et al., who stated that GFAP expression in healthy rats was limited in GCL, NFL, and INL [35, 36]. However, Duboc et al. [32] and Ponjavic and Andréasson [37] found increased GFAP immunoreactivity with VGB treatment. Lewis et al. and Xue et al. stated that in retinal diseases, GFAP is strongly expressed in Muller cells and can be considered a guide to the presence of reactive glial cells [38-40]. In addition, for the finding regarding VEGF immunoreactivity, Dijk et al. [41] confirmed that VEGF expression increased under oxidative stress, ischemic-hypoxic, and pathological conditions. VEGF is the main regulator of vascular permeability, angiogenesis, and endothelial cell proliferation [42].

Furthermore, SYN, also known as the major synaptic vesicle protein p38 and being one of the synaptic function markers, was used as a guide to assess the synapse in OPL and IPL because any retinal injury may cause alteration of synapse and consequently affect visual function [41]. The mild positive reaction of SYN in OPL and IPL in control and VGB/MSCs groups agreed with Dan et al. [25]. Although retinal ganglion cells death and thinning of the inner part of



the retina were found in VGB group, we found that SYN was upregulated as agreed by McKay et al. [43]. Moreover, Dan et al. [25] confirmed the same finding regarding SYN in a high intraocular pressure rat model.

However, synapsins are a family of proteins that have long been implicated in regulating synaptic neurotransmitter release. Synaptic proteins have been investigated in several photoreceptor degeneration animal models. One of these studies reported synapsin upregulation in the IPL of purkinje cell degeneration [44], consistent with our results for synapsin gene expression, which was upregulated in the retinal tissues of VGB treated group. This is consistent with the finding by Dagar et al. [28] reported enhanced synaptic protein levels in both bipolar and amacrine cells imply that synaptic activity in bipolar and amacrine cells is increased following photoreceptors loss.

As previously proved, increased vascular permeability is tightly associated with the reduced tight junction proteins in diabetic retinas [45]. As regarding to expression of occludin which is indispensable to tight junction integrity in endothelial cells and is the main constituents of the vascular permeability barrier, there was significant reduction in occludin expression in the VGB group. This point allows hUBC-MSCs homing in the retina and after treatment there was upregulation of occludin with repair to the retinal barrier. This finding agreed with Yu et al. [46], who highlighted that MSCs significantly upregulated the expression of occludin and reduces microvascular permeability [47]. Bamforth et al. [48] have verified that intravitreal injection of IL-1 $\beta$  causes breakdown of the vascular blood retinal barrier (BRB). Moreover, IL-1 $\beta$  and IL-6 indirectly cause the increase of retinal vascular permeability through inducing the expression of VEGF, which is known to be a key molecule leading to BRB breakdown in diabetes [49].

Moreover, VGB group showed significant upregulation in pro-apoptotic BAX expression and significant downregulation in the anti-apoptotic Bcl-2 expression compared to the control group; however, these results were reversed in VGB/MSCs group. This copes with Duboc et al. [32], who reported photoreceptor apoptosis in VGB-treated rats. In addition, comparable to our results, Meng et al. [50] and Li et al. [51] suggested that human adipose stem cells can suppress BAX, BAK, and caspase-3 expressions, which may contribute to their neuroprotective effects. Furthermore, Arnhold et al. [52] stated that MSCs could prolong photoreceptor survival in the rhodopsin knockout mouse and provide evidence of

a therapeutic benefit in retinitis pigmentosa. These results were consistent with Zhang and Wang [53] who stated that subretinal injection of bone marrow-MSCs caused photoreceptor apoptosis inhibition by released neurotrophic factors.

BDNF and NGF retinal expression exhibited a significant decrease in VGB group compared to control group, which was reversed in VGB/MSCs group. These results were also verified by a study of porcine retinal cells and human MSCs, suggesting that MSCs produce BDNF [54-56]. Li et al. [57] have demonstrated that MSCs transplantation offers the advantage of expressing various trophic factors as BDNF for at least four weeks. In contrast, Jindal et al. [58] disclosed that real-time data showed decreased expression of glial cell derived neurotrophic factor, ciliary neurotrophic factor, and BDNF after MSCs transplantation compared to injury. Moreover, Xu et al. [59] found that *NGF* gene expression was enhanced in differentiated MSCs, suggesting a higher potential of differentiated MSCs for regenerating diseased retinal tissue.

In conclusion, MSCs administration could be a suitable therapeutic line to ameliorate vigabatrin induced retinopathy. However, recurrence or retinal degeneration due to continuous usage of vigabatrin may occur.

## ORCID

Ayat Mahmoud Domouky:

<https://orcid.org/0000-0001-7516-629X>

Walaa M. Samy: <https://orcid.org/0000-0002-1542-1727>

Walaa A. Rashad: <https://orcid.org/0000-0001-7291-3798>

## Author Contributions

Conceptualization: AMD. Data acquisition: AMD, WMS, WAR. Data analysis or interpretation: AMD, WAR. Drafting of the manuscript: AMD, WMS. Critical revision of the manuscript: AMD, WMS, WAR. Approval of the final version of the manuscript: all authors.

## Conflicts of Interest

No potential conflict of interest relevant to this article was reported.

## Acknowledgements

Special thanks to Anatomy Department, Faculty of Medicine, Zagazig University. Many thanks to Zagazig University Animal House Department and Scientific Medical Research Center.

## References

- Holan V, Palacka K, Hermankova B. Mesenchymal stem cell-based therapy for retinal degenerative diseases: experimental models and clinical trials. *Cells* 2021;10:588.
- Semeraro F, Cancarini A, dell'Omo R, Rezzola S, Romano MR, Costagliola C. Diabetic retinopathy: vascular and inflammatory disease. *J Diabetes Res* 2015;2015:582060.
- Shaw PX, Stiles T, Douglas C, Ho D, Fan W, Du H, Xiao X. Oxidative stress, innate immunity, and age-related macular degeneration. *AIMS Mol Sci* 2016;3:196-221.
- van Norren D, Vos JJ. Light damage to the retina: an historical approach. *Eye (Lond)* 2016;30:169-72.
- Singh D, Jethani SL, Dubey A. Vigabatrin induced cell loss in the cerebellar cortex of albino rats. *J Clin Diagn Res* 2013;7:2555-8.
- Barrett D, Yang J, Sujirakul T, Tsang SH. Vigabatrin retinal toxicity first detected with electroretinographic changes: a case report. *J Clin Exp Ophthalmol* 2014;5:1000363.
- Ben-Menachem E. Mechanism of action of vigabatrin: correcting misperceptions. *Acta Neurol Scand Suppl* 2011;(192):5-15.
- Chan K, Hoon M, Pattnaik BR, Ver Hoeve JN, Wahlgren B, Gloe S, Williams J, Wetherbee B, Kiland JA, Vogel KR, Jansen E, Salomons G, Walters D, Roulet JB, Gibson KM, McLellan GJ. Vigabatrin-induced retinal functional alterations and second-order neuron plasticity in C57BL/6J mice. *Invest Ophthalmol Vis Sci* 2020;61:17.
- Yang J, Naumann MC, Tsai YT, Tosi J, Erol D, Lin CS, Davis RJ, Tsang SH. Vigabatrin-induced retinal toxicity is partially mediated by signaling in rod and cone photoreceptors. *PLoS One* 2012;7:e43889.
- Ravindran J, Blumbergs P, Crompton J, Pietris G, Waddy H. Visual field loss associated with vigabatrin: pathological correlations. *J Neurol Neurosurg Psychiatry* 2001;70:787-9.
- Hawker MJ, Astbury NJ. The ocular side effects of vigabatrin (Sabril): information and guidance for screening. *Eye (Lond)* 2008;22:1097-8.
- Waterhouse EJ, Mims KN, Gowda SN. Treatment of refractory complex partial seizures: role of vigabatrin. *Neuropsychiatr Dis Treat* 2009;5:505-15.
- Riikonen R, Renner-Primec Z, Carmant L, Dorofeeva M, Holody K, Szabo I, Krajnc BS, Wohlrab G, Sorri I. Does vigabatrin treatment for infantile spasms cause visual field defects? An international multicentre study. *Dev Med Child Neurol* 2015;57:60-7.
- Durbin S, Mirabella G, Buncic JR, Westall CA. Reduced grating acuity associated with retinal toxicity in children with infantile spasms on vigabatrin therapy. *Invest Ophthalmol Vis Sci* 2009;50:4011-6.
- Hou HY, Liang HL, Wang YS, Zhang ZX, Wang BR, Shi YY, Dong X, Cai Y. A therapeutic strategy for choroidal neovascularization based on recruitment of mesenchymal stem cells to the sites of lesions. *Mol Ther* 2010;18:1837-45.
- Achyut BR, Varma NR, Arbab AS. Application of umbilical cord blood derived stem cells in diseases of the nervous system. *J Stem Cell Res Ther* 2014;4:1000202.
- Chen T, Wang F, Wu M, Wang ZZ. Development of hematopoietic stem and progenitor cells from human pluripotent stem cells. *J Cell Biochem* 2015;116:1179-89.
- Nancarrow-Lei R, Mafi P, Mafi R, Khan W. A systemic review of adult mesenchymal stem cell sources and their multilineage differentiation potential relevant to musculoskeletal tissue repair and regeneration. *Curr Stem Cell Res Ther* 2017;12:601-10.
- Ding SLS, Kumar S, Mok PL. Cellular reparative mechanisms of mesenchymal stem cells for retinal diseases. *Int J Mol Sci* 2017;18:1406.
- Jammoul F, Wang Q, Nabbout R, Coriat C, Duboc A, Simonutti M, Dubus E, Craft CM, Ye W, Collins SD, Dulac O, Chiron C, Sahel JA, Picaud S. Taurine deficiency is a cause of vigabatrin-induced retinal phototoxicity. *Ann Neurol* 2009;65:98-107.
- Laitinen A, Laine J. Isolation of mesenchymal stem cells from human cord blood. *Curr Protoc Stem Cell Biol* 2007;Chapter 2:Unit 2A.3.
- Shehata AS, Mohamed DA, Hagraas SM, El-Beah SM, Elnegriss HM. The role of hesperidin in ameliorating retinal changes in rats with experimentally induced type 1 diabetes mellitus and the active role of vascular endothelial growth factor and glial fibrillary acidic protein. *Anat Cell Biol* 2021;54:465-78.
- Suvarna SK, Layton C, Bancroft JD. Bancroft's theory and practice of histological techniques. 7th ed. Edinburgh: Churchill Livingstone Elsevier; 2013.
- Chen H, Weber AJ. Expression of glial fibrillary acidic protein and glutamine synthetase by Müller cells after optic nerve damage and intravitreal application of brain-derived neurotrophic factor. *Glia* 2002;38:115-25.
- Dan C, Jian-Bin T, Hui W, Le-Ping Z, Jin Z, Ju-Fang H, Xue-Gang L. Synaptophysin expression in rat retina following acute high intraocular pressure. *Acta Histochem Cytochem* 2008;41:173-8.
- Youssef NS, Said AM. Immunohistochemical expression of CD117 and vascular endothelial growth factor in retinoblastoma: possible targets of new therapies. *Int J Clin Exp Pathol* 2014;7:5725-37.
- El-Gohari K, Bahei-Eldin I, Habib E, Saad S, Rady H, Said A. Neuroprotection of the rat's retinal ganglion cells against glutamate-induced toxicity. *J Egypt Ophthalmol Soc* 2016;109:135-44.
- Dagar S, Nagar S, Goel M, Cherukuri P, Dhingra NK. Loss of photoreceptors results in upregulation of synaptic proteins in

- bipolar cells and amacrine cells. *PLoS One* 2014;9:e90250.
29. Liu X, Wang D, Liu Y, Luo Y, Ma W, Xiao W, Yu Q. Neuronal-driven angiogenesis: role of NGF in retinal neovascularization in an oxygen-induced retinopathy model. *Invest Ophthalmol Vis Sci* 2010;51:3749-57.
  30. Tao Y, Ding L, Yao A, Yang Z, Yang Q, Qin L, Yu L, Gao Y, Huang YF, Li Z, Teng D. Intravitreal delivery of Ab-crySTALLIN ameliorates N-methyl-N-nitrosourea induced photoreceptor degeneration in mice: an *in vivo* and *ex vivo* study. *Cell Physiol Biochem* 2018;48:2147-60.
  31. Vogel KR, Pearl PL, Theodore WH, McCarter RC, Jakobs C, Gibson KM. Thirty years beyond discovery--clinical trials in succinic semialdehyde dehydrogenase deficiency, a disorder of GABA metabolism. *J Inher Metab Dis* 2013;36:401-10.
  32. Duboc A, Hanoteau N, Simonutti M, Rudolf G, Nehlig A, Sahel JA, Picaud S. Vigabatrin, the GABA-transaminase inhibitor, damages cone photoreceptors in rats. *Ann Neurol* 2004;55:695-705.
  33. Jammoul F, Dégardin J, Pain D, Gondouin P, Simonutti M, Dubus E, Caplette R, Fouquet S, Craft CM, Sahel JA, Picaud S. Taurine deficiency damages photoreceptors and retinal ganglion cells in vigabatrin-treated neonatal rats. *Mol Cell Neurosci* 2010;43:414-21.
  34. Wang QP, Jammoul F, Duboc A, Gong J, Simonutti M, Dubus E, Craft CM, Ye W, Sahel JA, Picaud S. Treatment of epilepsy: the GABA-transaminase inhibitor, vigabatrin, induces neuronal plasticity in the mouse retina. *Eur J Neurosci* 2008;27:2177-87.
  35. Gaucher D, Arnault E, Husson Z, Froger N, Dubus E, Gondouin P, Dherbécourt D, Dégardin J, Simonutti M, Fouquet S, Benahmed MA, Elbayed K, Namer IJ, Massin P, Sahel JA, Picaud S. Taurine deficiency damages retinal neurones: cone photoreceptors and retinal ganglion cells. *Amino Acids* 2012;43:1979-93.
  36. Zhou L, Wang H, Luo J, Xiong K, Zeng L, Chen D, Huang J. Regulatory effects of inhibiting the activation of glial cells on retinal synaptic plasticity. *Neural Regen Res* 2014;9:385-93.
  37. Ponjavic V, Andréasson S. Multifocal ERG and full-field ERG in patients on long-term vigabatrin medication. *Doc Ophthalmol* 2001;102:63-72.
  38. Lewis GP, Fisher SK. Up-regulation of glial fibrillary acidic protein in response to retinal injury: its potential role in glial remodeling and a comparison to vimentin expression. *Int Rev Cytol* 2003;230:263-90.
  39. Sethi CS, Lewis GP, Fisher SK, Leitner WP, Mann DL, Luthert PJ, Charteris DG. Glial remodeling and neural plasticity in human retinal detachment with proliferative vitreoretinopathy. *Invest Ophthalmol Vis Sci* 2005;46:329-42.
  40. Xue LP, Lu J, Cao Q, Hu S, Ding P, Ling EA. Müller glial cells express nestin coupled with glial fibrillary acidic protein in experimentally induced glaucoma in the rat retina. *Neuroscience* 2006;139:723-32.
  41. Dijk F, Bergen AA, Kamphuis W. GAP-43 expression is up-regulated in retinal ganglion cells after ischemia/reperfusion-induced damage. *Exp Eye Res* 2007;84:858-67.
  42. Ferrara N. Molecular and biological properties of vascular endothelial growth factor. *J Mol Med (Berl)* 1999;77:527-43.
  43. McKay JS, Steele SJ, Ahmed G, Johnson E, Ratcliffe K. An antibody panel for immunohistochemical analysis of the retina in Davidson's-fixed, paraffin-embedded eyes of rats. *Exp Toxicol Pathol* 2009;61:91-100.
  44. Marchena M, Lara J, Aijón J, Germain F, de la Villa P, Velasco A. The retina of the PCD/PCD mouse as a model of photoreceptor degeneration. A structural and functional study. *Exp Eye Res* 2011;93:607-17.
  45. Barber AJ, Antonetti DA. Mapping the blood vessels with paracellular permeability in the retinas of diabetic rats. *Invest Ophthalmol Vis Sci* 2003;44:5410-6.
  46. Yu C, Yang K, Meng X, Cao B, Wang F. Downregulation of long noncoding RNA MIAT in the retina of diabetic rats with tail-vein injection of human umbilical-cord mesenchymal stem cells. *Int J Med Sci* 2020;17:591-8.
  47. Mao F, Wu Y, Tang X, Wang J, Pan Z, Zhang P, Zhang B, Yan Y, Zhang X, Qian H, Xu W. Human umbilical cord mesenchymal stem cells alleviate inflammatory bowel disease through the regulation of 15-LOX-1 in macrophages. *Biotechnol Lett* 2017;39:929-38.
  48. Bamforth SD, Lightman SL, Greenwood J. Interleukin-1 beta-induced disruption of the retinal vascular barrier of the central nervous system is mediated through leukocyte recruitment and histamine. *Am J Pathol* 1997;150:329-40.
  49. Qaum T, Xu Q, Jousen AM, Clemens MW, Qin W, Miyamoto K, Hassessian H, Wiegand SJ, Rudge J, Yancopoulos GD, Adams AP. VEGF-initiated blood-retinal barrier breakdown in early diabetes. *Invest Ophthalmol Vis Sci* 2001;42:2408-13.
  50. Meng HB, Gong J, Zhou B, Hua J, Yao L, Song ZS. Therapeutic effect of human umbilical cord-derived mesenchymal stem cells in rat severe acute pancreatitis. *Int J Clin Exp Pathol* 2013;6:2703-12.
  51. Li Z, Wang J, Gao F, Zhang J, Tian H, Shi X, Lian C, Sun Y, Li W, Xu JY, Li P, Zhang J, Gao Z, Xu J, Wang F, Lu L, Xu GT. Human adipose-derived stem cells delay retinal degeneration in royal college of surgeons rats through anti-apoptotic and VEGF-mediated neuroprotective effects. *Curr Mol Med* 2016;16:553-66.
  52. Arnhold S, Absenger Y, Klein H, Addicks K, Schraermeyer U. Transplantation of bone marrow-derived mesenchymal stem cells rescue photoreceptor cells in the dystrophic retina of the rhodopsin knockout mouse. *Graefes Arch Clin Exp Ophthalmol* 2007;245:414-22.
  53. Zhang Y, Wang W. Effects of bone marrow mesenchymal stem cell transplantation on light-damaged retina. *Invest Ophthalmol Vis Sci* 2010;51:3742-8.
  54. Labrador-Velandia S, Alonso-Alonso ML, Di Lauro S, García-Gutiérrez MT, Srivastava GK, Pastor JC, Fernández-Bueno I. Mesenchymal stem cells provide paracrine neuroprotective resources that delay degeneration of co-cultured organotypic neuroretinal cultures. *Exp Eye Res* 2019;185:107671.
  55. Wang S, Lu B, Girman S, Duan J, McFarland T, Zhang QS, Grompe M, Adamus G, Appukuttan B, Lund R. Non-invasive

- stem cell therapy in a rat model for retinal degeneration and vascular pathology. PLoS One 2010;5:e9200.
56. Jindal N, Mukhopadhyay A, Anand A. The emerging role of stem cells in ocular neurodegeneration: hype or hope? Mol Cell Biochem 2012;365:65-76.
57. Li N, Li XR, Yuan JQ. Effects of bone-marrow mesenchymal stem cells transplanted into vitreous cavity of rat injured by ischemia/reperfusion. Graefes Arch Clin Exp Ophthalmol 2009;247:503-14.
58. Jindal N, Banik A, Prabhakar S, Vaiphie K, Anand A. Alteration of neurotrophic factors after transplantation of bone marrow derived Lin-ve stem cell in NMDA-induced mouse model of retinal degeneration. J Cell Biochem 2017;118:1699-711.
59. Xu W, Wang X, Xu G, Guo J. Light-induced retinal injury enhanced neurotrophins secretion and neurotrophic effect of mesenchymal stem cells *in vitro*. Arq Bras Oftalmol 2013;76:105-10.